MDPI

Article

Advances in Drinking Water Treatment through Piloting with UF Membranes

Federico A. Leon-Zerpa [1],*, Jenifer Vaswani-Reboso [1], Tomas Tavares [2], Alejandro Ramos-Martín [1] and Carlos A. Mendieta-Pino [1]

1   Departamento de Ingeniería de Procesos, Universidad de las Palmas de Gran Canaria, 35017 Las Palmas de Gran Canaria, Spain
2   Faculdade de Ciências e Tecnologia, Escola de Ciências Agrárias e Ambientais, Universidade de Cabo Verde, Praia CP 7943-010, Cape Verde
*   Correspondence: federicoleon@perezvera.com

Abstract: This manuscript presents the advances of a pilot testing, located in Spain, using ultrafiltration (UF) membranes to supply drinking water. These results could be extended to the islands of the Macaronesia area, for instance, Azores, Madeira, Canaries, and Cape Verde. The UF project targeted by the pilot activity is a refurbishment of an existing installation. The existing installation is located at a higher altitude, thus drinking water could be supplied to most of the island without further pumping, reducing the carbon footprint, ecological footprint, and energy consumption. The raw water is soft surface water (mainly of rainwater origin) coming from a dam. On the islands of Macaronesia, water is a scarce resource in high demand. Therefore, this is a technically and economically viable business opportunity with a promising future for isolated water treatment systems to produce drinking water on islands. The Macaronesia area is formed by volcanic islands with a small surface in the Atlantic Ocean, so usually there is not enough space for conventional technology and only a compact UF can be used. The raw water quality is not satisfactory and the municipality receives many complaints from end users, thus a potable water plant with UF membranes is in high demand to supply drinking water of good quality. Membrane processes can be categorized into various, related methods, three of which include the following: pore size, molecular weight cut-off, and operating pressure. Regarding the obtained results, the UF system successfully produced excellent filtrate quality with turbidity readings on average less than 0.03 NTU; furthermore, membrane instantaneous flux of 90 Lmh at 14 °C is achievable with long-term stability under various feed water conditions, peak operations are available at 105 Lmh without a large impact on the filtration performance of the modules, and CIP is only to be performed if the TMP increase reaches the terminal point.

Keywords: ultrafiltration; advances; water treatment; drinking water

![check for updates]

1. Introduction

This paper shows the results of a new project concerning a pilot testing, located in Spain, using ultrafiltration (UF) membranes to supply potable water. It could be extended to the islands of the Macaronesia area (Azores, Madeira, Canaries, and Cape Verde). The UF project targeted by the pilot activity is a refurbishment of an existing installation. The existing installation is located at a higher altitude, thus drinking water could be supplied to most of the island without further pumping, reducing the carbon footprint, ecological footprint, and energy consumption [1–4].

The raw water is soft surface water (mainly of rainwater origin) coming from a dam, located 8 km away from the drinking water facility. The raw water reaches the facility via an 8 km long gravitational tunnel across a mountain [5–9]. After the raw water intake, carbonate slurry is dosed to increase the alkalinity and hardness. Based on the explanation of local operators, coagulation is very difficult with the raw water. Because of the chemical

characteristics of the water, it has a low tendency for the formation of flocs [10–14]. The next treatment step is a lamella clarifier. Originally, the facility was designed and operated with two lamella clarifiers. However, owing to the high slope of the site location, one of the clarifiers collapsed because of the unstable foundation. Currently, the system runs with only clarifier, which doubles the filtration velocity and appears to be the major root of all operational troubles. As the facility is surrounded by houses, there is no space for conventional technology, and only a compact UF can be used [15–18].

The water quality is not satisfactory and the municipality receives many complaints from end users. After the clarifier, the water is further treated in sand filters. The plan is to place the UF technology on the current location of the existing sand filters. This document summarizes the findings of this pilot study program [19–21]. Regarding the filtration spectrum, filtration is defined as the separation of two or more components from a fluid stream. In conventional usage, it usually refers to the separation of solid, insoluble particles from liquid or gaseous streams. Membrane filtration extends this application further to include the separation of dissolved solids in liquid streams, hence membrane processes in water treatment are commonly used to remove various materials, ranging from salts to microorganisms. The most commonly employed membrane processes and the filtration ranges in which they operate are presented in Figure 1 below [22–25].
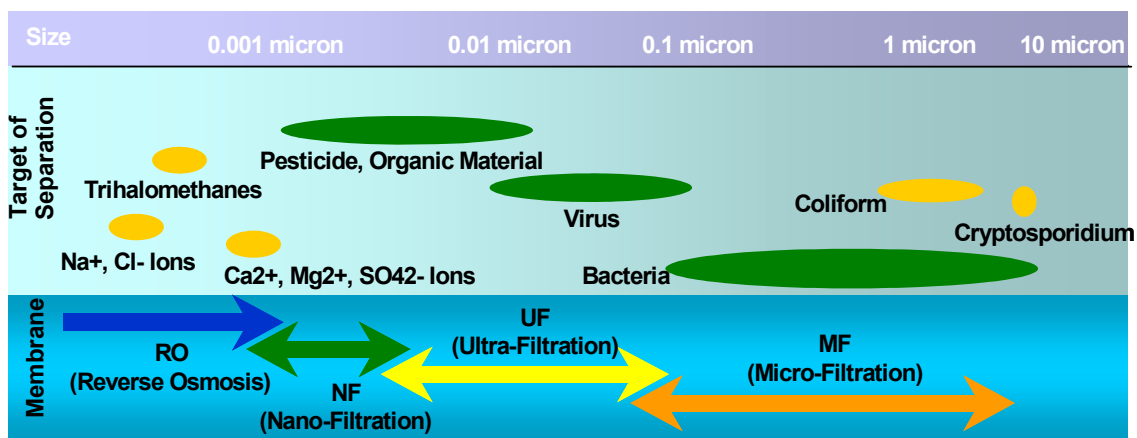

Figure 1. Membrane processes and filtration ranges.

Membrane processes can be categorized into various, related methods, three of which include the following: pore size, molecular weight cut-off, and operating pressure. As the pore size becomes smaller or the molecular weight cut-off decreases, the pressure applied to the membrane for the separation of water from other material generally increases. The water treatment objectives will determine the basis on which a process is selected [26–29].

The pilot activity was performed with different raw water scenarios, which were artificially created by the local operator team. The dates of the different scenarios are presented in Table 1.

Bentonite is used as a non-adsorbent source of turbidity. The performance of bentonite was tested in raw water/bentonite and it acts as a coagulation aid for water treatment.

The objectives of this pilot study were as follows:

- To determine the effectiveness of the ultrafiltration system to treat raw feed water at the drinking water treatment plant.
- To demonstrate that the ultrafiltration system produces a high-quality filtrate, which has a turbidity <0.1 NTU.
- To define operational flux and in situ cleaning protocols.
- To define operating parameters for a full-scale ultrafiltration system, including chemical dosing, membrane flux, and recovery.

Table 1. Different scenarios of the operations and periods.

Scenario	Date
untreated raw water	From 6 March 2018
re-mineralized water with chlorine and adding 0.5 mg/L of Fe	From 20 March 2018
re-mineralized water with chlorine and adding 1 mg/L of Fe	From 26 March 2018
re-mineralized water pre-chlorination and 10 mg/L PAX	From 3 April 2018
re-mineralized water pre-chlorination and PAX 30 mg/L	From 9 April 2018
re-mineralized water pre-chlorination and PAX 50 mg/L	From 17 April 2018
re-mineralized water pre-chlorination and PAX 10 mg/L and 0.5 mg/L of iron	From 27 April 2018
re-mineralized water pre-chlorination and adding bentonite until 3.5 NTU	From 3 May 2018
re-mineralized water pre-chlorination and adding bentonite until 7 NTU	From 8 May 2018
re-mineralized water pre-chlorination and adding bentonite until 10 NTU	From 10 May 2018
re-mineralized water pre-chlorination and adding bentonite 10 NTU + 10 mg/L de PAX + 0.5 mg/L Fe	14 May 2018 to 21 May 2018
normal operational regime with re-mineralized raw water	After 1 May 2018

2. Materials and Methods

Feed water is pumped to the membrane modules at a feed pressure in the range between 2 bars and a maximum feed pressure of 3 bar. Particulate matter, including Virus, Giardia cysts, and Cryptosporidium oocysts, remain on the outside of the membrane fibre, while permeate enters through to the inside (lumen) of the hollow fibres and exits the top port of the membrane module. The filtration cycle continues for 30 min (in this application), after which the particulate/suspended solids are removed from the module during the backwash cycle. In the backwash cycle, the feed to the module stops and permeate from the backwash tank is directed into the hollow fibres for 45 s. After the concentrated solution is sent to drain, feed water fills the module, air bubbles scour the membranes for 30 s, and then the module is drained again. The overall backwash cycle requires approximately 2.8 min [30–39].

In this application, NO sodium hypochlorite was added to the backwash water (filtrate).

Total maintenance cleans (TMCs) were not performed during this pilot study. Because the raw water organics are low, it was decided to implement only chemical cleaning (CIP) instead of regular and frequent TMC [40–45].

CIP cleaning is normally performed when the trans-membrane pressure (TMP) approaches the maximum of 2 bars. CIP cleaning is similar to TMC, except the soak period is longer and the chlorine concentration is higher. The typical duration for CIP cleaning is 4–6 h.

For this pilot study, CIP cleaning was not required because of a TMP issue, but it was performed once to keep the membrane in clean condition between the different phases.

The membrane characteristics are as follows.

Type: HFU2020-AN (cross-flow filtration).
Membrane Material: PVDF (polyvinylidene fluoride)
Nominal Pore Size: μm 0.01
Outer Membrane Surface Area: m^2 (ft^2) 72 (775)
Operating Temperature Range: °C (°F) 0–40 (32–104)
pH Range During Filtration: 1–10
pH Range During Cleaning: 0–12

The pump characteristics and operation parameters are as follows.

Maximum Feed Water/Filtrate Flow: m^3/h (gpm) 12 (53)

Maximum Backwash Flow: m^3/h (gpm) 13.5 (59)
Maximum Air Flow: Nm^3/h (scfm) 9.0 (5.3)
Maximum Inlet Pressure: bar 3
Maximum Backwash Pressure: bar 3
Normal Operating Transmembrane Pressure: bar 0–2
Diameter: mm (in) 216 (8.5)
Length: mm (ft) 2160 (7.087)
Weight:
Full of Water: kg (lbs) 92 (203)
After Draining: kg (lbs) 49 (108)
Casing: uPVC
Cap: uPVC
Potting: epoxy resin
O-ring: EPDM

This module is used in vertical position, mainly for saving space in the installation. The performance of the module is the same when used in a horizontal or vertical position, but, for a huge installation, it is more suitable to use it in a vertical position.

Throughout the course of this pilot study, data logger data were gathered along with field data. The data logger data consisted of date, time, raw water temperature, feed flowrate, feed pressure, filtrate pressure, and calculated trans-membrane pressure, as well as permeate turbidity. The data were collected every minute and, from the data, instantaneous flux and the temperature-corrected permeability were calculated and graphed.

The main characteristic of the PVDF material of these UF modules is the resistance of the membrane, in addition to the fouling effect produced by its pore size.

In terms of permeation and rejection, in order to obtain high-performing membranes with better antifouling resistance, it is crucial to make the correct selection of nanocomposite materials according to their properties, for instance, composition, surface charge, size, type of material, surface area, material loading, hydrophilic/hydrophobic nature, and so on [46–48].

3. Results

The raw water analysis before pilot testing is presented in Table 2 and that during pilot testing is presented in the Table 3.

Table 2. Raw water analysis before pilot testing.

Parameter	Unit	Data		
		Min.	**Avg.**	**Max.**
Total suspended solids (TSS)	mg/L	n/a	2	5
Turbidity	NTU		4	10
pH	-	5.8	n/a	7.3
Temperature	°C	8	14	25

The operational and laboratory results began being recorded in March 2018 and operations were completed in June 2018. During this time period, three separate phases were examined. The first was the demonstration phase, where the pilot unit was operated with low filtration flux in order to gain operational insights into the suitability of the raw water for fouling.

In phase 2 of the operation, the full-scale plant design was simulated with moderate operational flux under various raw water conditions (the raw water quality was artificially adjusted).

Owing to the low feed water turbidities, it was decided to increase the operational flux in phase 3 in order examine the performance of the UF modules.

Table 3. Raw water analysis measured during the pilot testing.

Parameter	Unit	Data		
		Min.	**Avg.**	**Max.**
Colour	degree	0	11.3	38
Free chlorine	mg/L	0	0.7	1.5
Turbidity	NTU	0.2	5.1	50.1
Total iron (Fe)	mg/L	0	0.47	3
Aluminium (Al)	mg/L	0.016	0.52	1.9
Alkalinity (as $CaCO_3$)	mEq/L	0.3	1.8	3.0
Conductivity	µS/cm	21.6	57.9	78.6
Oxidability	Mg O_2/L	0.5	1.2	2.4
Total manganese (Mn)	mg/L	0.0007	0.023	0.181
Hardness (as $CaCO_3$)	mEq/L	0.2	2.0	6.2
pH	-	5.4	7	7.7
Coliforms	CFU/mL	0	0.1	1

In this pilot study, the HFU2008-N test module was used. The test module uses the same membrane fibers as the larger HFU2020-N module, which is recommended for the full-scale plant. The test module is a similar height (2.0 m) to HFU2020-N (2.1 m), but the membrane surface area is lower. The test module has a surface area of 11.5 m^2 while HFU2020-N has a surface area of 72 m^2. Because the height of the fibers is similar and the membrane chemistry is the same, the pilot test results accurately reflect how the HFU2020-N module will perform in the full-scale plant.

3.1. Phase 1 (Demonstration Phase)

During the demonstration phase, from 8 March to 23 April 2018, all operating parameters were well within the design guidelines. The pilot unit operated in filtration mode for 30 min and then backwashed for 45 s. For the BW, no chlorine was used.

In summary, during the first two months of the pilot study, the HFU pilot unit operated with the following parameters:

○ Instantaneous flux rate of 45–50 L/m^2h.
○ Average feed temperature of 13 °C.
○ Operating trans-membrane pressure (TMP) of 0.42 to 0.5 bar.
○ Average permeate turbidity of <0.03 NTU (peaks during the BW procedure due to the presence of bubbles in the measuring cells).
○ Temperature-corrected permeability (20 °C) ranging from 90 to 95 L/(hm^2bar) (in the 45–50 L/m^2h range).

The graphs demonstrating the performance trends noted above are attached for further clarification in Appendix A: Performance Graphs Phase 1 (operational graphs are only available from 18 April).

The operating guidelines state that the TMP should range from 0.14 bar to 1.4 bar and CIP cleaning should be performed before 2 bar is reached.

In the appendix figures, there are some sudden changes in TMP caused by changes in the feed water quality. From Figure A6 (in Appendix B), it is evident that, from 31 March to 1 June 2018, a stable TMP of less than 0.28 bar was observed. It should be noted that maintenance cleans were not included in the pilot study or in the full-scale design. From Figure 2, it is evident that the operation with this low flux value is very stable. Throughout the pilot test, the unit faced difficulties in flow control and required manual inputs. The flowrate was manually checked and adjusted accordingly, which resulted in slight variation in the flow curves. The backwash flowrate was manually checked and the throttle valve was

adjusted in order to reach the design set-point, which was $1.1\times$ filtration flux. Figure A2, in Appendix A, presents the flow and temperature variation in phase 1, which was in the range between 12 and 14 °C. In Figures A3–A5, it is evident that the permeate quality is excellent. The turbidity readings are consistently at 0.02 NTU, except where the BW procedure occurred. Disturbance of the turbidity measurement occurred during the BW procedure. During the BW procedure, the turbidity measuring cell was disturbed by the presence of small bubbles, which resulted in short turbidity peaks. The regularly occurring turbidity peaks are thus not related to the deterioation in permeate quality, but only to this disturbance of the measurement. The graphs in Figures A3–A5 provide evidence that turbidity peaks (marked with red cells) only occurred during the BW procedure. The typical turbidity reading during the filtration period is presented in Figure 2.

Figure 2. Typical turbidity reading during the filtration period.

3.2. Phase 2—Operation at 90 L/m^{2}h + Simulating Turbidity Peaks by Bentonite Dosing

During the demonstration phase, the average feed turbidities were less than 4 NTU. Because the maximum feed turbidity in the full-scale plant is likely to have peaks up to 10 NTU, phase 1 was designed to simulate 6–10 NTU peaks by bentonite dosing.

Before this artificial peak simulation, the unit was operated at a design point with 90 l/m^{2}h instantaneous flux and at a recovery of 93.5%.

Therefore, the feed water particulate was concentrated 20 times.

Concentration Factor = 1/(1-recovery) = 1/(1 − 0.935) = 15

With a feed turbidity of 2 NTU at the end of the filtration cycle (30 min), the likely turbidity would be 2 × 15 = 30 NTU. With a feed turbidity of 10 NTU at 93.5% recovery, the concentrated feedwater would have a turbidity of 10 × 15 = 150 NTU.

The concentration is also visually observable in the reject stream, as shown in Figures 3 and 4.

Figure 3. Feed, permeate, and reject water.

Figure 4. Reject water after 30 min sedimentation.

Summary of operation at 90 L/m^{2}h:

○ Instantaneous flux rate of 90 L/m^{2}h.
○ Average feed temperature of 14 °C.
○ Operating trans-membrane pressure (TMP) of 0.7 to 0.8 bar.
○ Average permeate turbidity of <0.03 NTU (peaks during the BW procedure due to the presence of bubbles in the measuring cells).
○ Temperature-corrected permeability (20 °C) ranging from 131 to 150 L/m^{2}hbar at 90 L/m^{2}h.

The graphs demonstrating the performance trends noted above are attached for further clarification in Appendix B: Performance Graphs Phase 2.

From Appendix B Figure A6, it is evident that the operation with 90 L/m^{2}h in the temperature range of 13–15 °C is very stable. This operational regime can be maintained without chemical cleaning. There is more information in Figures A7–A13.

By the beginning of May 2018, bentonite dosing was applied. From Figure 4, it is remarkable that the system reacts with the increase in TMP. Nevertheless, this increase in TMP was easily kept under control with the increase in BW time. The BW time was increased from 45 s to 60 s and the air scouring was increased from 30 s to 50 s. This impacted the overall recovery, reducing it from 93.5% to 92.4%. This intensification of the BW procedure resulted in a much better de-concentration, and thus contributed greatly to the stabilization of the operation at 90 L/m^{2}h, without implementing any chemical cleans.

Summary of the operation with bentonite:

○ Instantaneous flux rate of 90–95 L/m^{2}h (because of some technical issues, the feed flow control was not fully stable).
○ Average feed temperature of 14 °C.
○ Operating trans-membrane pressure (TMP) of 1 to 0.5 bar.
○ Average permeate turbidity of <0.03 NTU (peaks during the BW procedure due to the presence of bubbles in the measuring cells).
○ Temperature-corrected permeability (20 °C) ranging from 105 to 220 L/m^{2}hbar at 90 l/m^{2}h.

3.3. Phase 3—Operation at 105 L/m^{2}h

In the final phase of the pilot, the unit was operated at 1200 L/h, which corresponds to an instantaneous flux of 105 L/m^{2}h. This rather short test period demonstrated that the operation is stable even in the case of 105 L/m^{2}h flux.

Summary of the operation with bentonite:

○ Instantaneous flux rate of 105 L/m^{2}h.
○ Average feed temperature increased to 17 °C.
○ Operating trans-membrane pressure (TMP) of 1 to 0.5 bar.
○ Average permeate turbidity of <0.03 NTU (peaks during the BW procedure due to the presence of bubbles in the measuring cells).
○ Temperature-corrected permeability (20 °C) ranging from 103 to 153 L/m^{2}hbar at 105 L/m^{2}h.

No chemical cleaning was necessary to maintain the operational conditions. The TMP was stabilised at 1.05 bar.

3.4. Cleaning Results

Regarding cleaning dangers, we have to take special precautions when handling chemicals during chemical cleaning. Safety gear such as safety glasses and protective gloves should be worn. If chemicals come into direct contact with your skin or your clothes, you should treat the affected area appropriately based on the SDS. Moreover, we cannot mix sodium hypochlorite with acid. Such a mixture generates toxic chlorine gas. Finally, we have to stop the operation whenever any anomaly occurs with the equipment; orange signs indicate an anomaly [45,46].

Otherwise, you may damage the modules or negatively affect the membrane performance. The only cleaning performed on the HFU pilot unit was a short CIP with sodium hypochlorite (850 ppm, 3 h) followed by a short acid-CIP (4200 ppm citric acid, 3 h). These cleanings were performed at the end of the demonstration phase in order to start effective testing on the design flux with clean membranes. As in the further period of the piloting the trans-membrane pressure did not rise above an acceptable level and therefore CIP cleaning was not required [47,48].

CIP cleaning is to be considered in the full-scale design as a consolidated and secure design approach. However, CIP is only to be performed if the increase in TMP reaches the terminal point.

4. Conclusions and Future Lines

This paper presents the results of a new project about a pilot testing, where a UF system was used to successfully produce excellent filtrate quality with turbidity readings on average less than 0.03 NTU.

Moreover, membrane instantaneous flux of 90 L/m^{2}h at 14 °C was achievable with long-term stability under various feed water conditions.

The pilot unit was operated with low filtration flux in order to gain operational insights into the suitability of the raw water for fouling. Moreover, peak operations are available at 105 L/m^{2}h without a large impact on the filtration performance of the modules.

CIP cleaning was considered in the full-scale design as a consolidated and secure design approach, but CIP is only to be performed if the increase in TMP reaches the terminal point.

Author Contributions: Conceptualization, F.A.L.-Z., C.A.M.-P. and A.R.-M.; methodology, F.A.L.-Z., C.A.M.-P. and A.R.-M.; validation, T.T. and J.V.-R.; formal analysis, T.T. and J.V.-R.; investigation, F.A.L.-Z., T.T. and J.V.-R.; data curation, T.T. and J.V.-R.; writing—original draft preparation, F.A.L.-Z., C.A.M.-P. and A.R.-M.; writing—review and editing, F.A.L.-Z.; visualization, T.T. and J.V.-R.; supervision, T.T. and J.V.-R.; project administration, F.A.L.-Z., C.A.M.-P., A.R.-M. and J.V.-R.; funding acquisition, F.A.L.-Z., T.T., J.V.-R. and J.V.-R. All authors have read and agreed to the published version of the manuscript.

Institutional Review Board Statement: Not applicable.

Appendix A

Performance Graphs Phase 1.
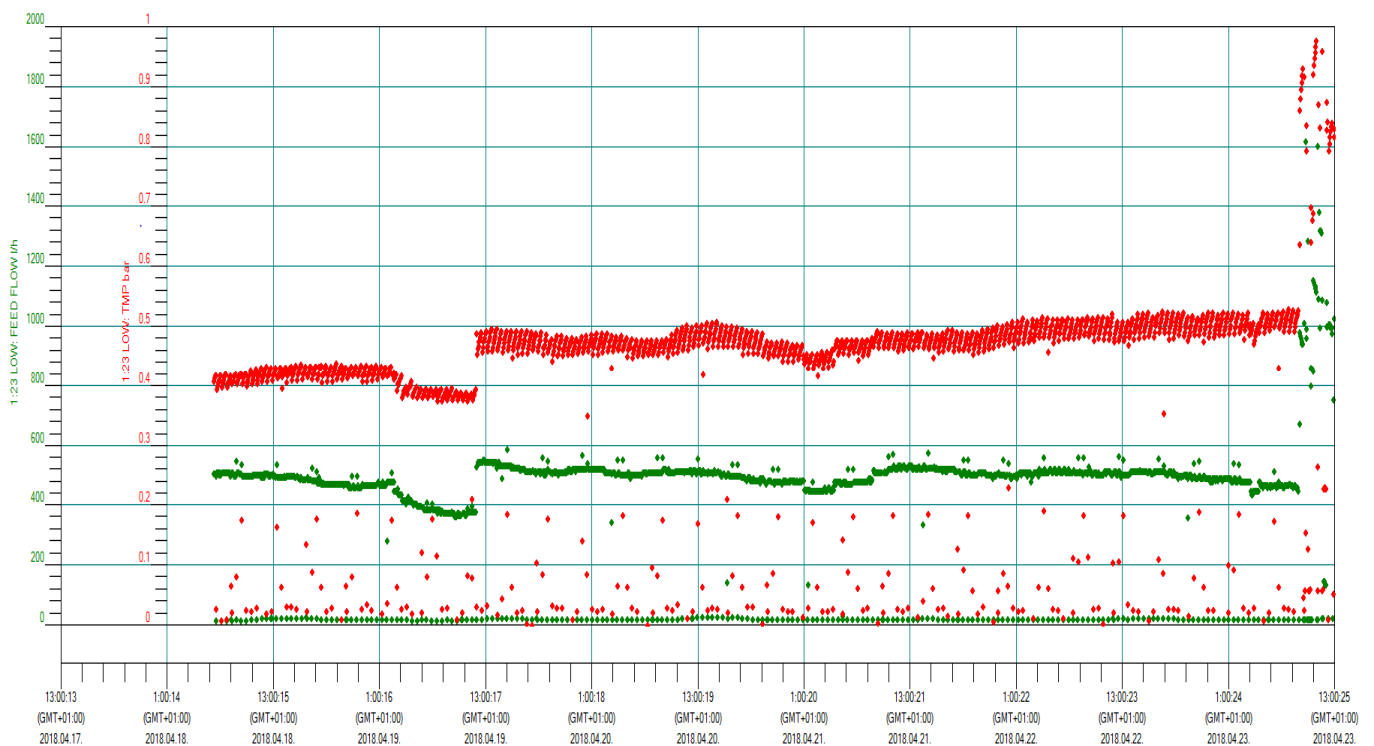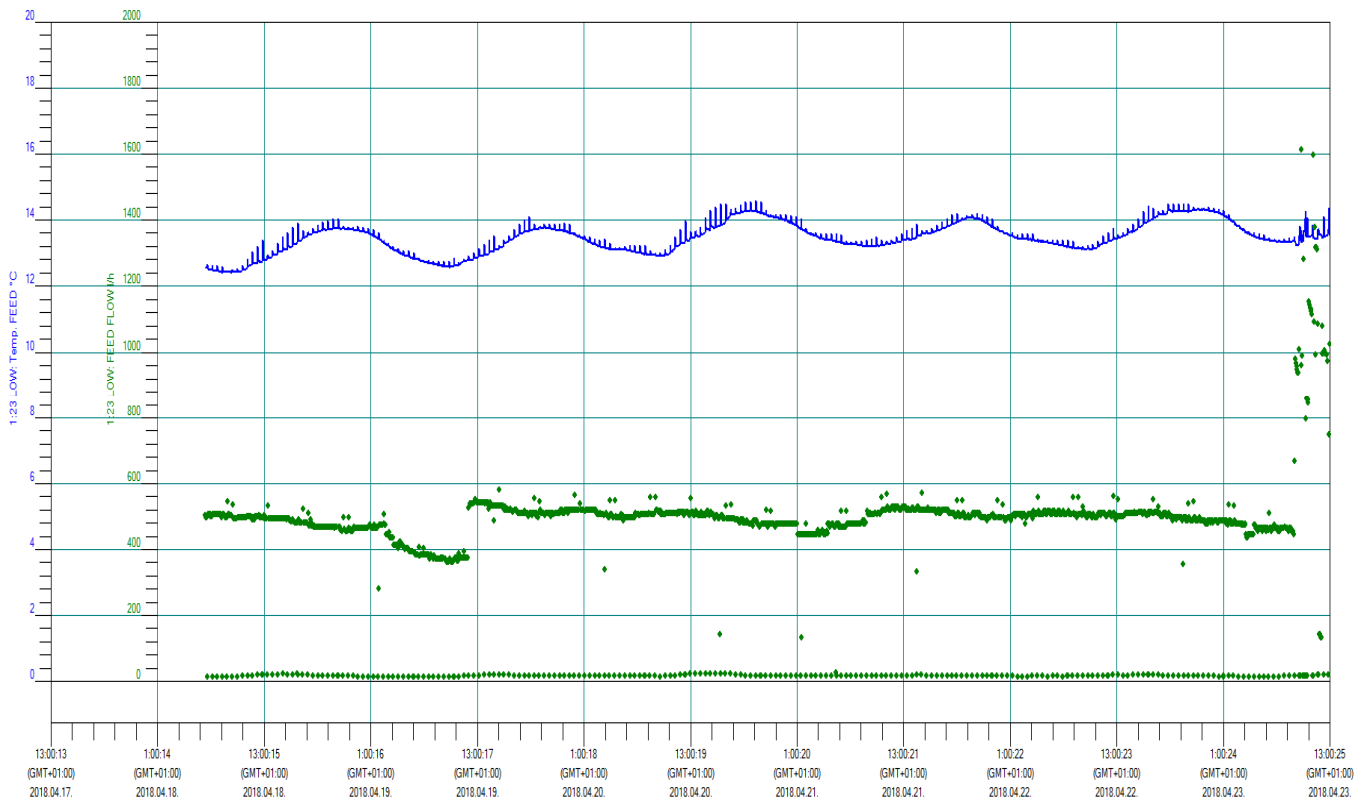

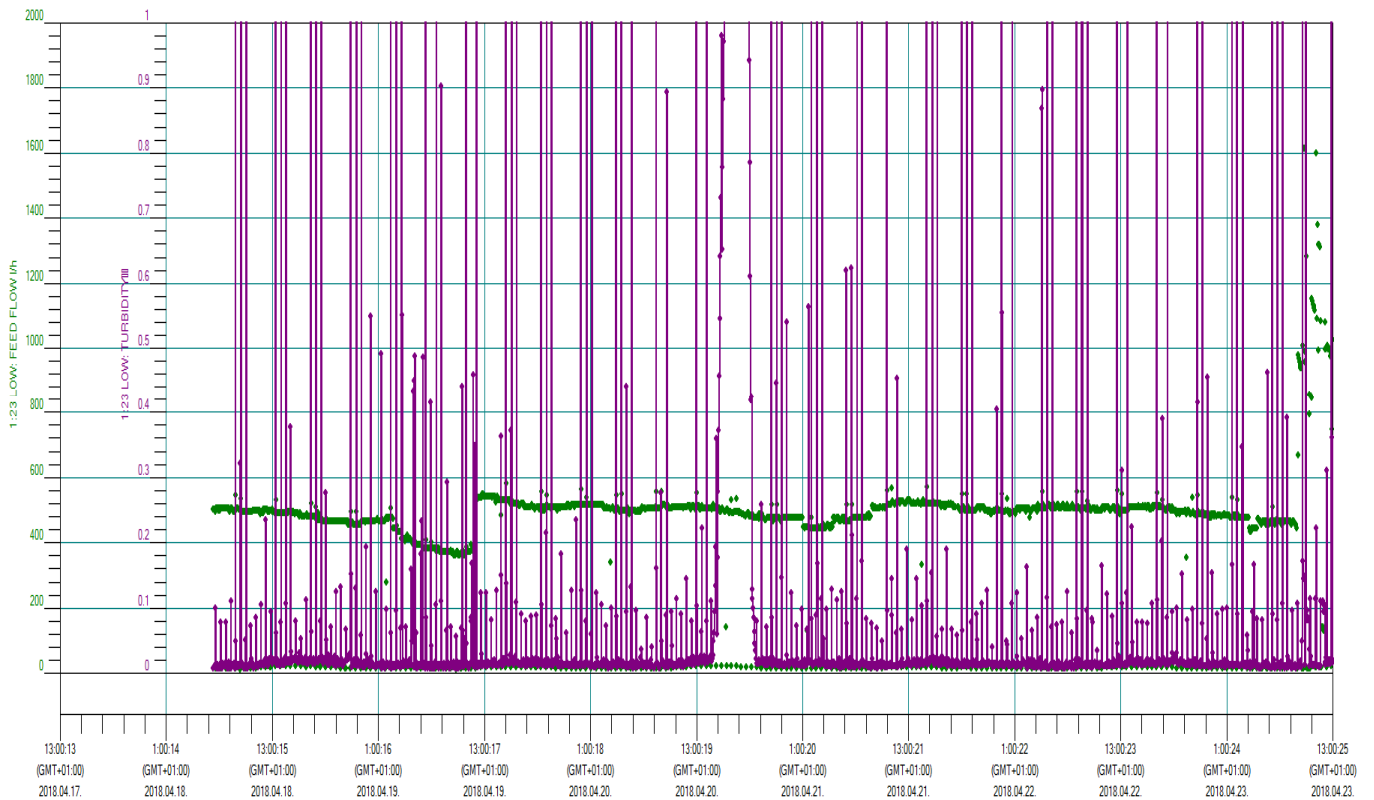**Figure A1.** Flow and TMP.

Figure A2. Flow and temperature.

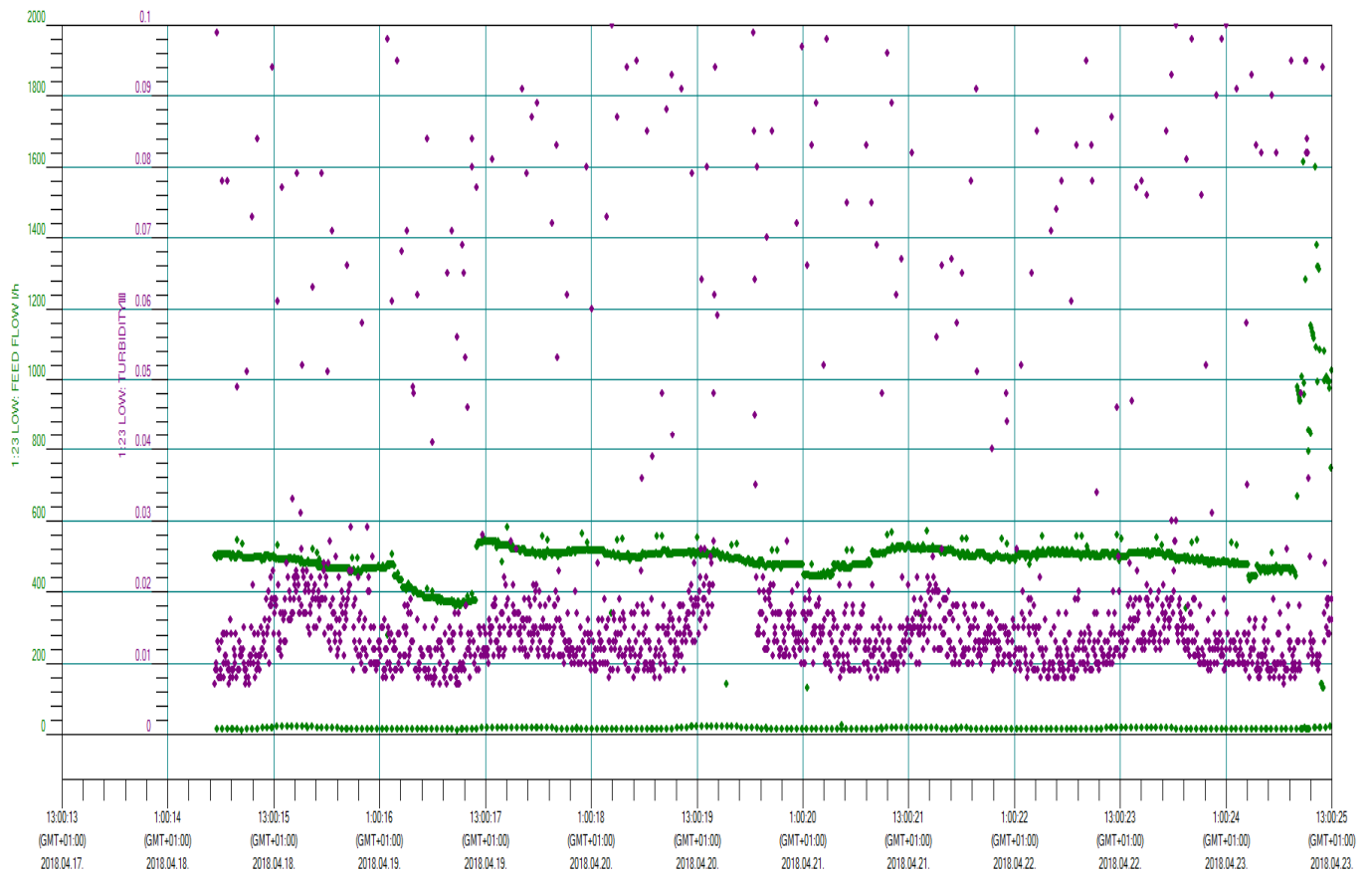**Figure A3.** Flow and permeate turbidity (low resolution).

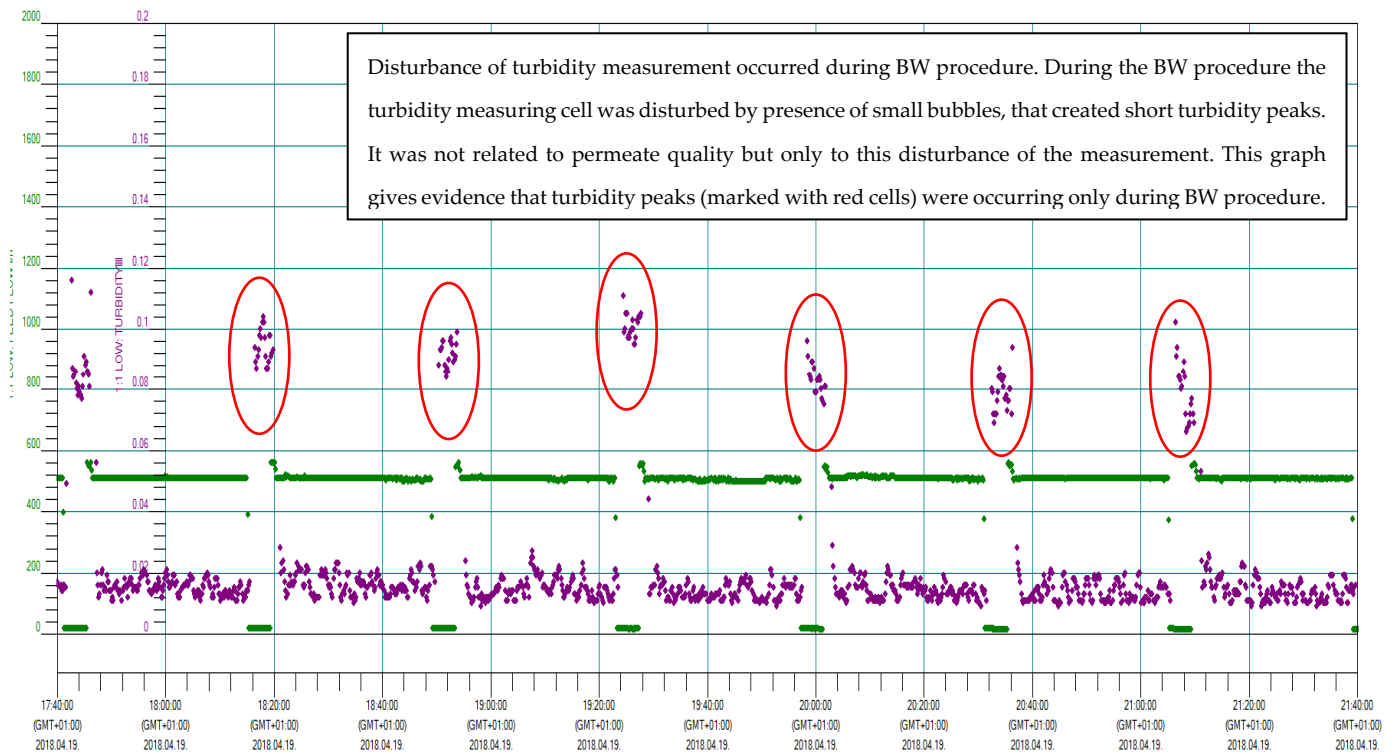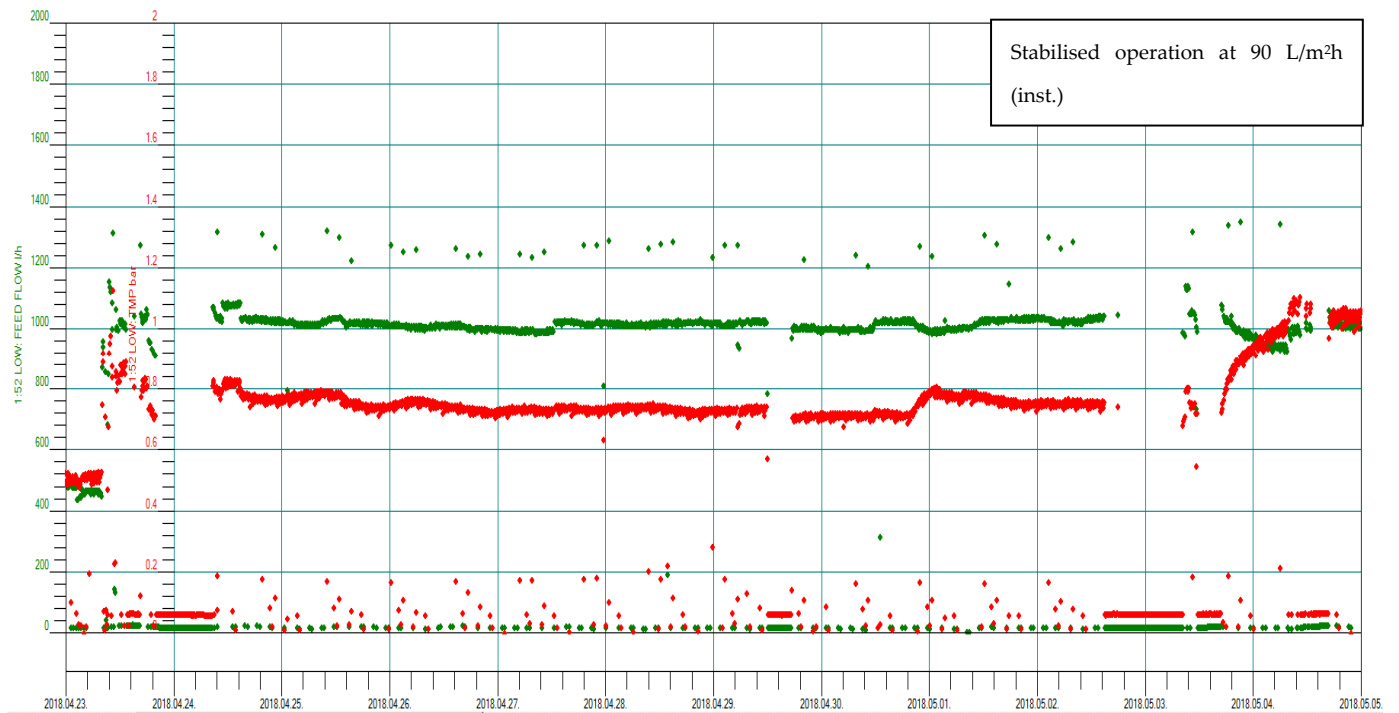**Figure A4.** Flow and permeate turbidity (medium resolution).

Disturbance of turbidity measurement occurred during BW procedure. During the BW procedure the turbidity measuring cell was disturbed by presence of small bubbles, that created short turbidity peaks. It was not related to permeate quality but only to this disturbance of the measurement. This graph gives evidence that turbidity peaks (marked with red cells) were occurring only during BW procedure.

Figure A5. Flow and permeate turbidity (high resolution).

Appendix B

Performance Graphs Phase 2.

> Stabilised operation at 90 L/m²h (inst.)
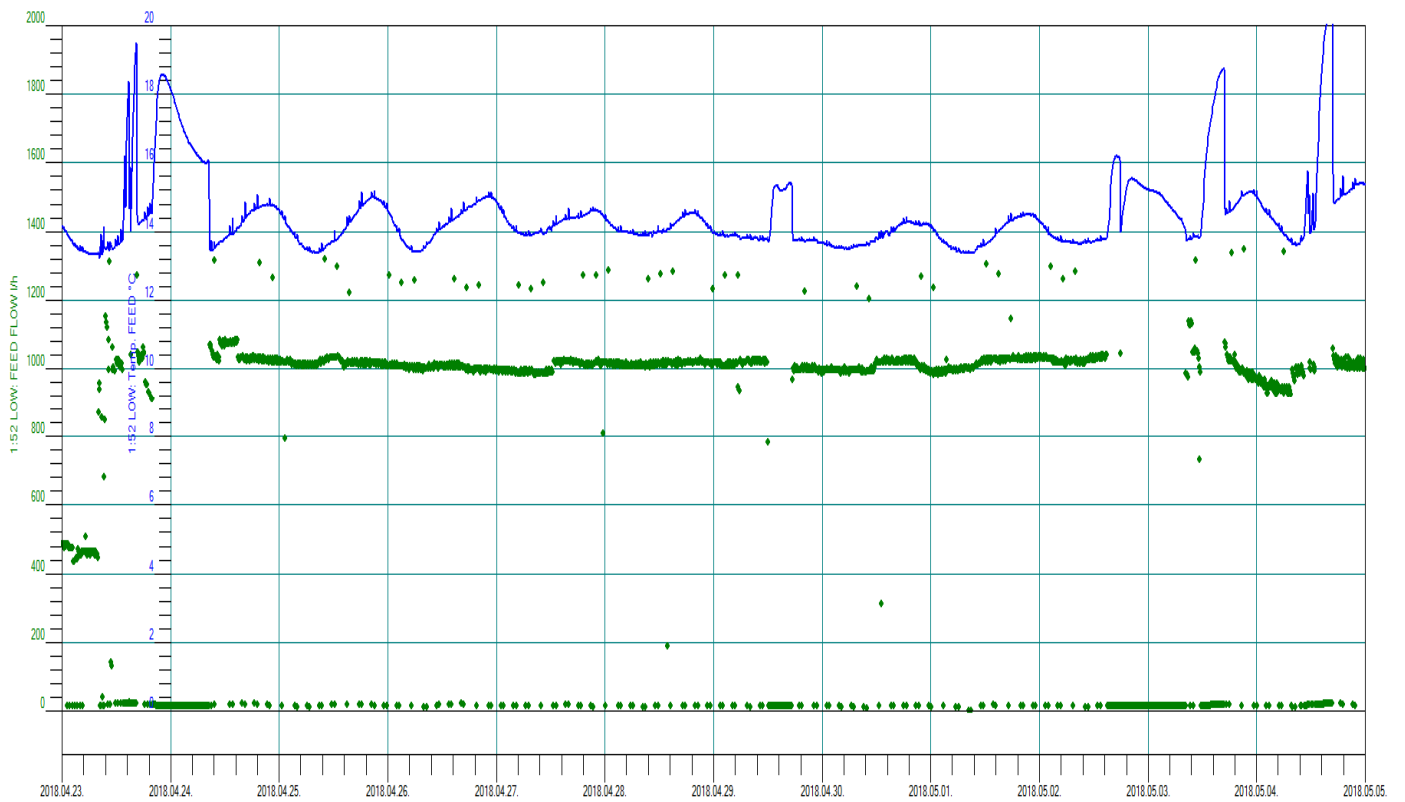
Figure A6. Flow and TMP.
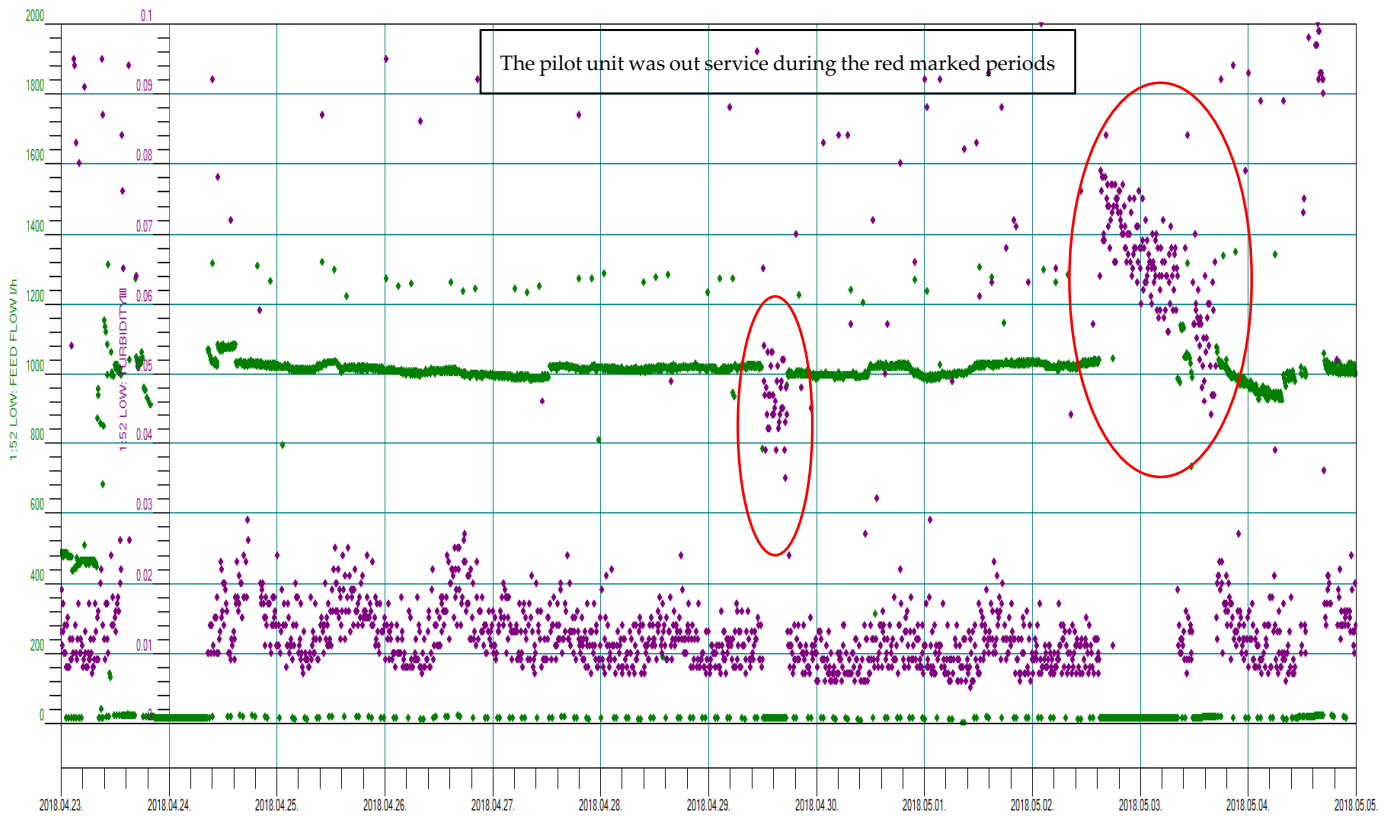

Figure A7. Flow and temperature.

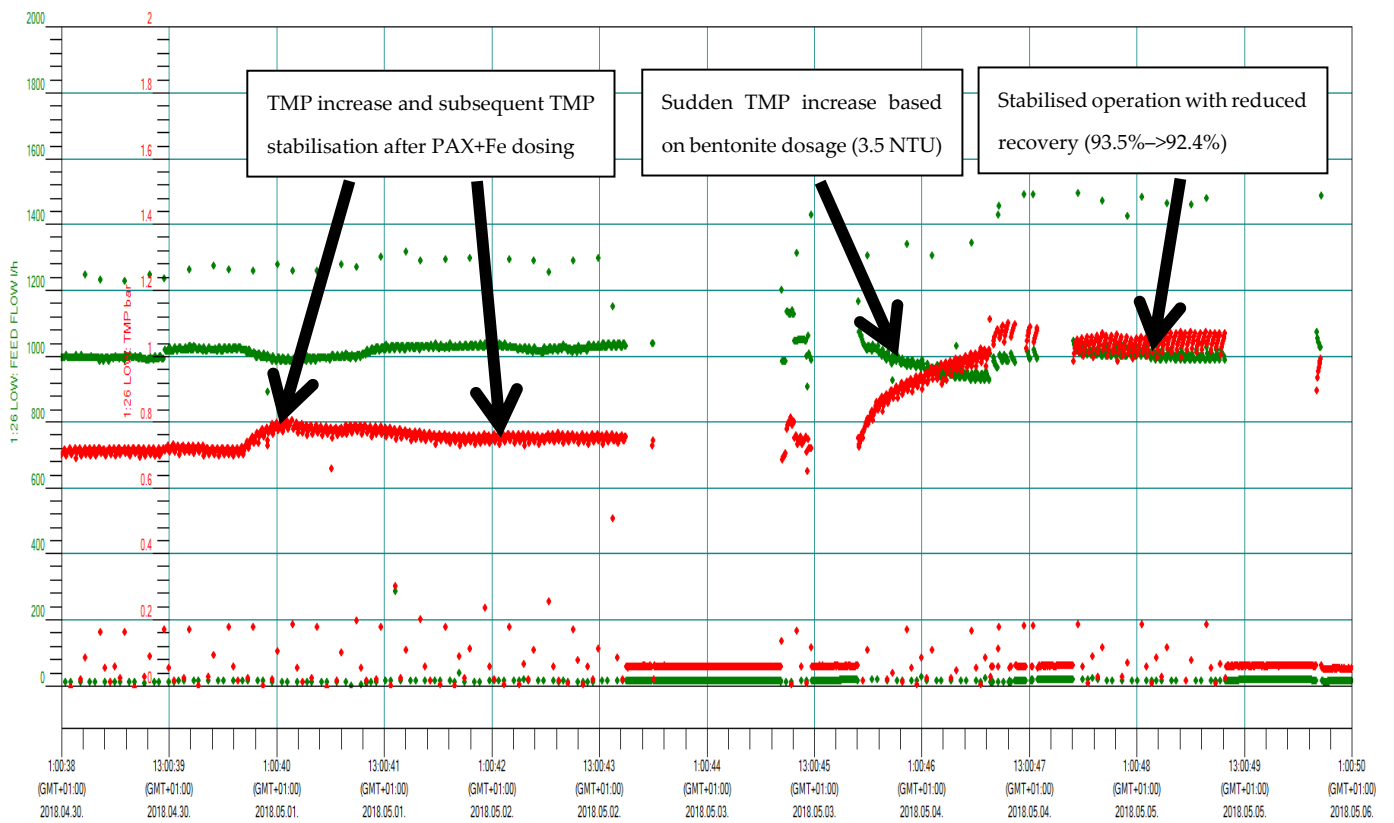**Figure A8.** Flow and permeate turbidity.

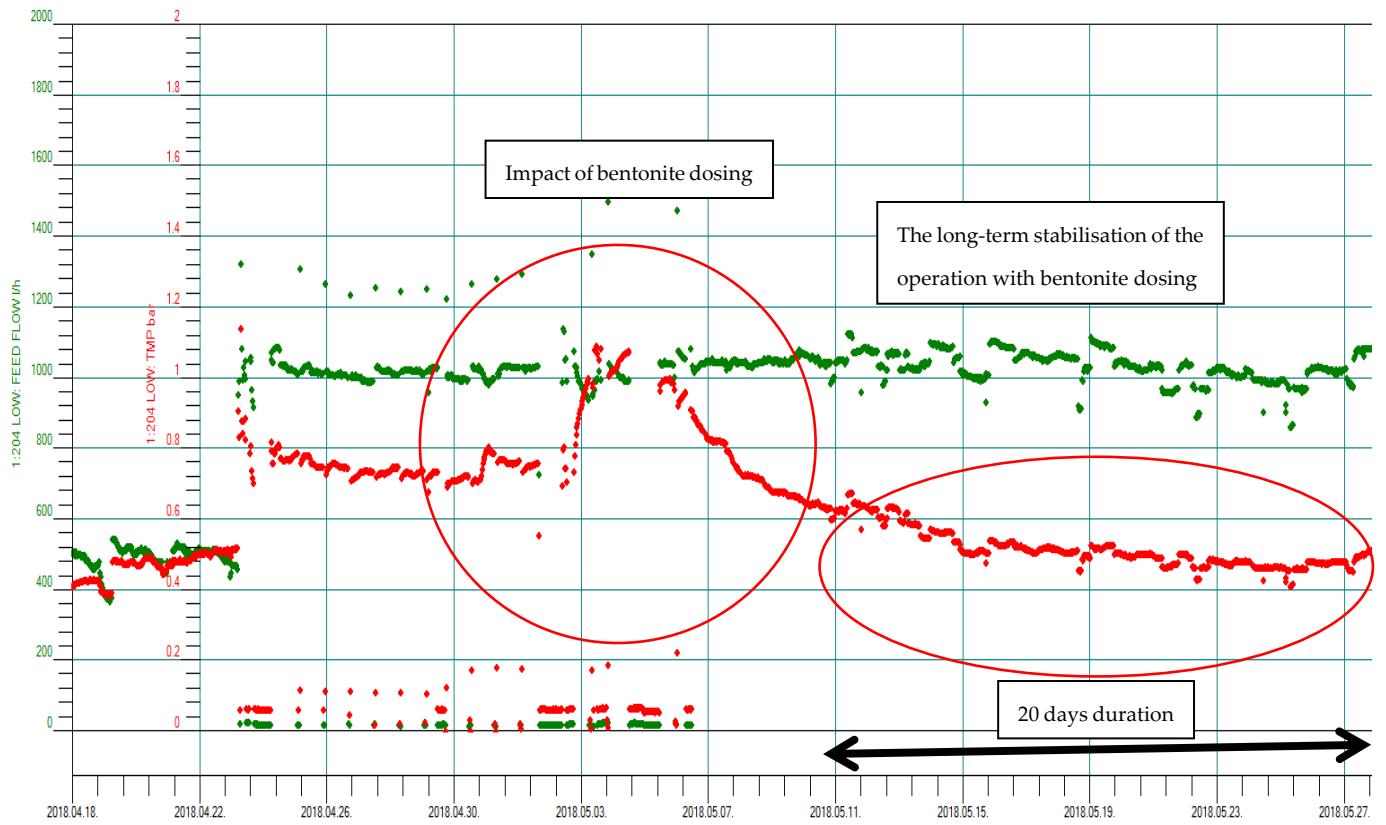**Figure A9.** Flow and TMP with bentonite dosing.

Figure A10. Flow and TMP—the impact of bentonite dosing.
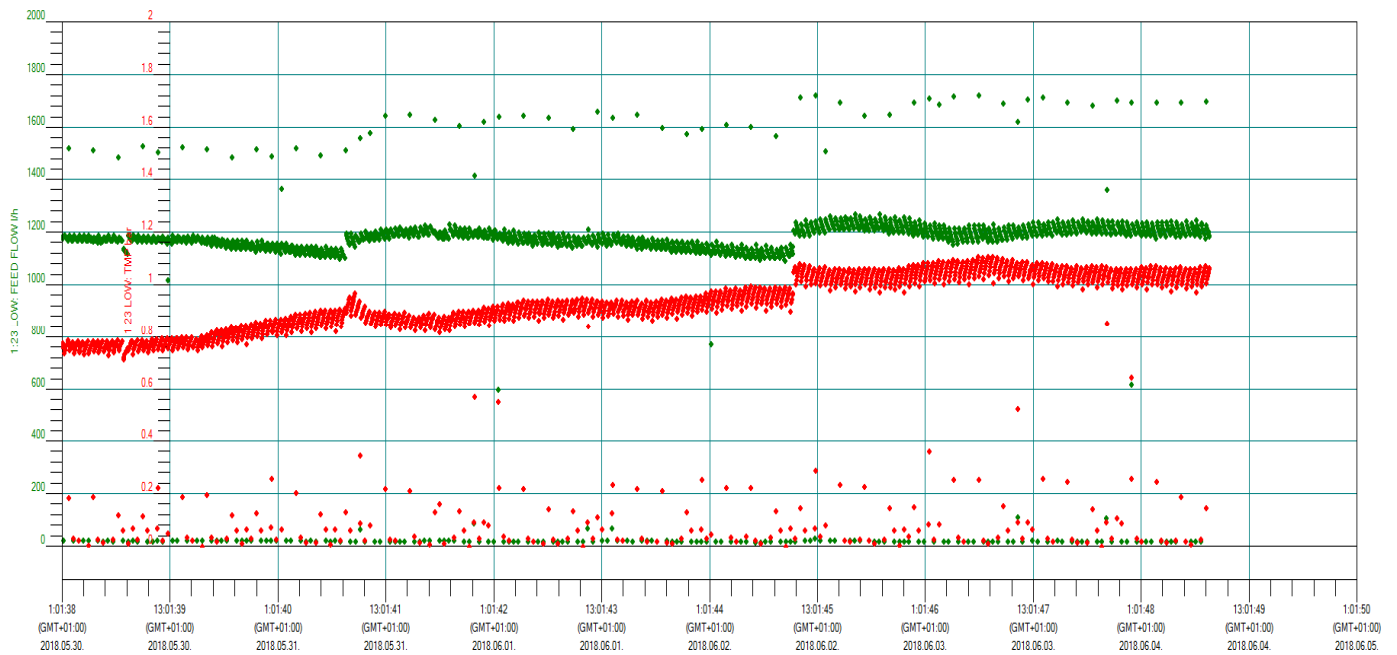
Appendix C

Performance Graphs Phase 3.

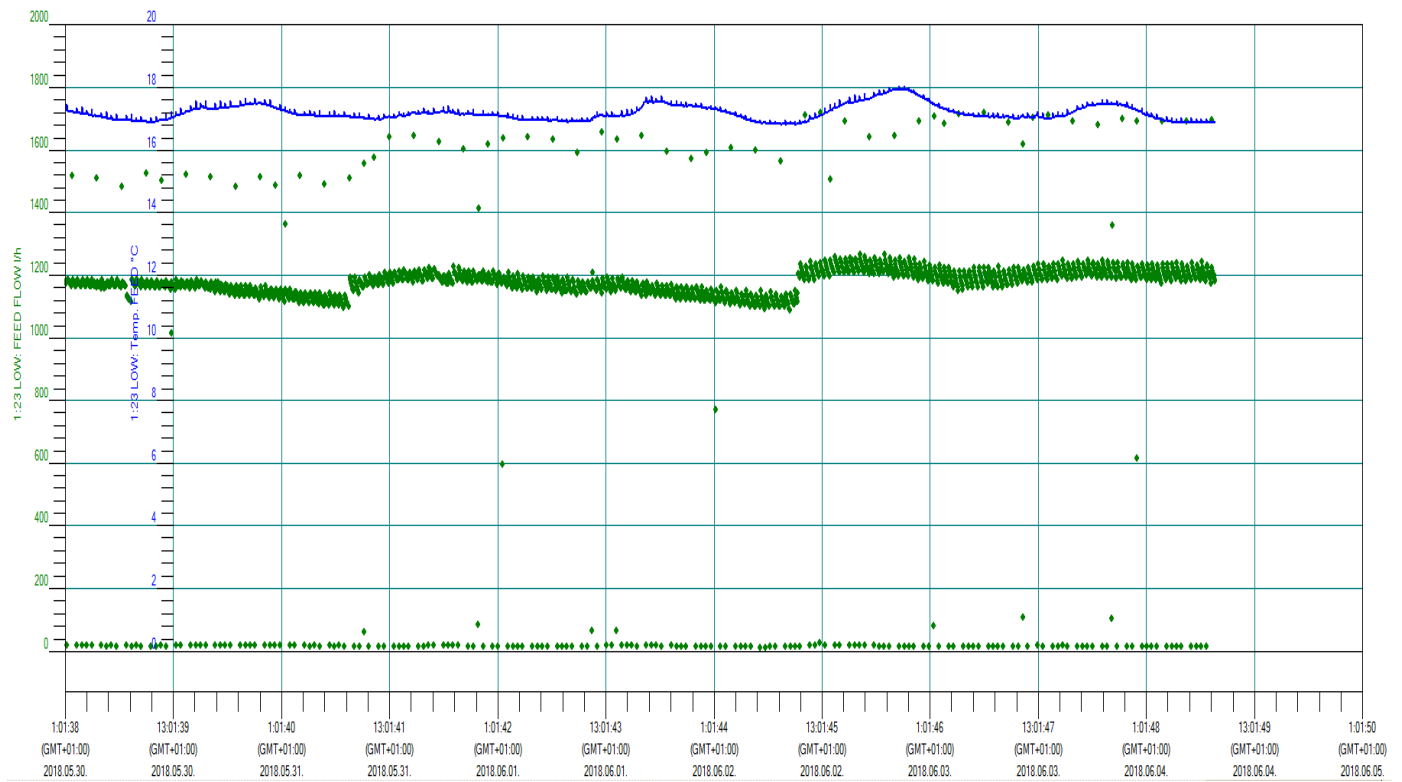**Figure A11.** Flow and TMP at 105 L/m²h.

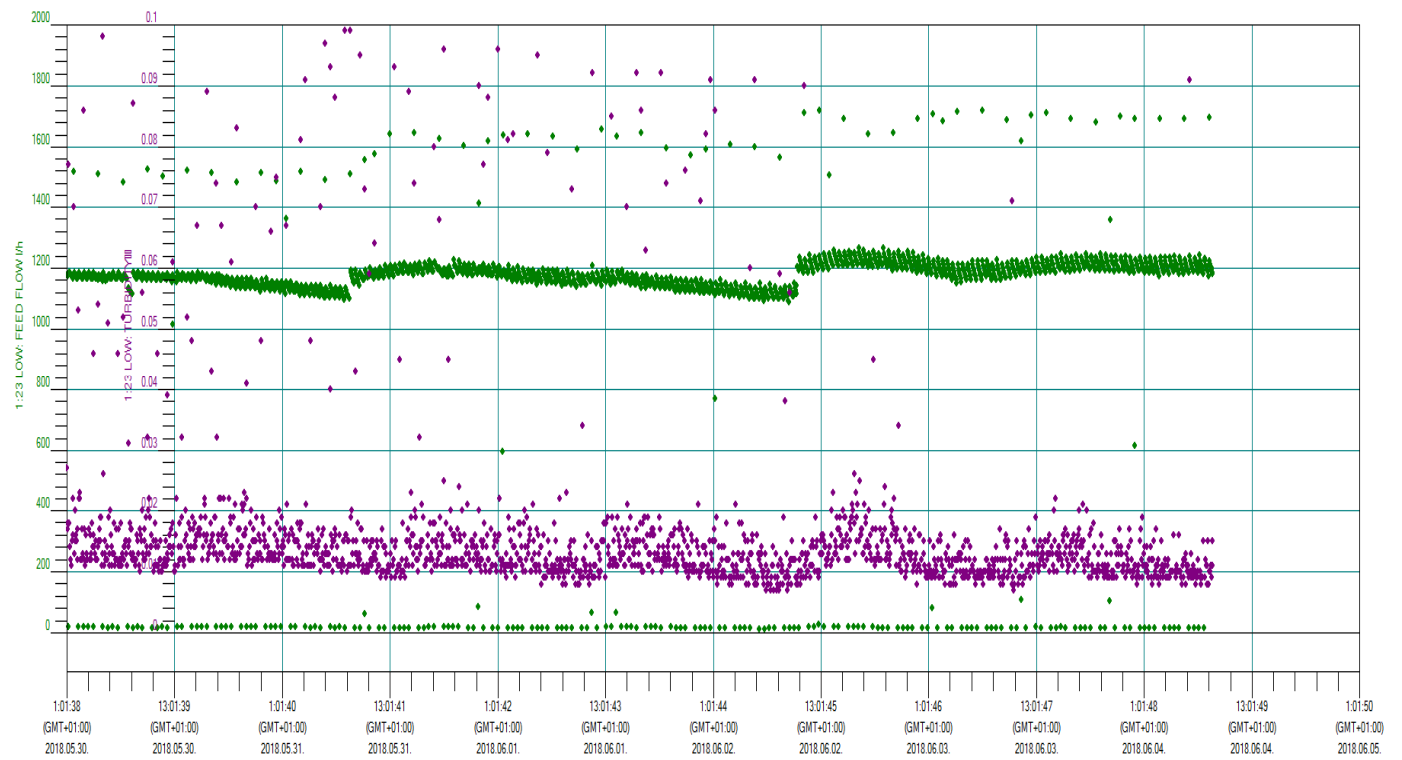**Figure A12.** Flow and temperature at 105 l/m^{2}h.

Figure A13. Flow and permeate turbidity at 105 L/m^{2}h.

References

1. Rajewska, P.; Janiszewska, J.; Rajewska, J. Integration of Ultra- and Nanofiltration for Potato Processing Water (PPW) Treatment in a Circular Water Recovery System. *Membranes* **2023**, *13*, 59. [CrossRef] [PubMed]
2. Tshindane, P.; Mamba, B.B.; Motsa, M.M.; Nkambule, T.T.I. Delayed Solvent–Nonsolvent Demixing Preparation and Performance of a Highly Permeable Polyethersulfone Ultrafiltration Membrane. *Membranes* **2023**, *13*, 39. [CrossRef]
3. Cano, G.; Moulin, P. Treatment of Boiler Condensate by Ultrafiltration for Reuse. *Membranes* **2022**, *12*, 1285. [CrossRef] [PubMed]
4. Kurihara, M. Seawater Reverse Osmosis Desalination. *Membranes* **2021**, *11*, 243. [CrossRef] [PubMed]
5. Ruiz-García, A.; Melián-Martel, N.; Nuez, I. Short Review on Predicting Fouling in RO Desalination. *Membranes* **2017**, *7*, 62. [CrossRef]
6. Silva, J.; Torres, P.; Madera, C. Reúso de aguas residuales domésticas en agricultura. Una revisión. *Rev. Agron. Colomb.* **2008**, *26*, 347–359.
7. World Health Organization—WHO. Wasstewater Use in Agricultura. In *WHO Guidelines for the Safe Use of Wastewater, Excreta and Greywater*; WHO: Paris, France, 2006; Volume II, p. 222.
8. WHO. World Health Organization—Water, Fact Sheet 391. Available online: http://www.who.int/mediacentre/factsheets/fs391/en/2014 (accessed on 5 August 2014).
9. Quist-Jensen, C.A.; Macedonio, F.; Drioli, E. Membrane technology for water production in agricultura: Desalination and wastewater reuse. *Desalination* **2015**, *364*, 17–32. [CrossRef]
10. Latorre, F.J.G.; Báez, S.O.P.; Gotor, A.G. Energy performance of a reverse osmosis desalination plant operating with variable pressure and flow. *Desalination* **2015**, *366*, 146–153. [CrossRef]
11. Kheriji, J.; Mnif, A.; Bejaoui, I.; Hamrouni, B. Study of the influence of operating parameters on boron removal by a reverse osmosis membrane. *Desalination Water Treat.* **2015**, *56*, 2653–2662. [CrossRef]
12. Schallenberg-Rodríguez, J.; Veza, J.M.; Blanco-Marigorta, A. Energy efficiency and desalination in Cape Verde. *Renew. Sustain. Energy Rev.* **2014**, *40*, 741–748. [CrossRef]
13. Zerpa, F.L.; Martín, A.R.; Pino, C.A.M. Prueba piloto de membranas de alta eficiencia para la optimización de sistemas de membranas en la planta de desalinización de Carboneras. *DYNA* **2021**, *96*, 260–263. [CrossRef]
14. Bosque Maurel, J.; Valenti, J.V. *Geografía De España*; Ariel: Barcelona, Spain, 2022; p. 10.
15. De España, G. Available online: https://administracion.gob.es/pag_Home/espanaAdmon/comoSeOrganizaEstado/ComunidadesAutonomas.html (accessed on 31 May 2021).
16. Morales Matos, G. Las Islas Canarias ¿Una Región Aislada? *Boletín de la A.G.E. N.* **2001**, *32*, 155.
17. Parlamento Europeo. Tratado De Funcionamiento De La Unión Europea (TFUE)—Artículos 349 Y 355—Las Regiones Ultra-periféricas (Rup). In *Fichas Técnicas Sobre La Unión Europea*; Parlamento Europeo: Strasbourg, France, 2016.
18. León-Zerpa, F.; Peñate-Suárez, B.; Roo-Filgueira, J.; Vaswani, J. Reutilización de elementos de ósmosis inversa de los procesos de desalación. *DYNA* **2021**, *96*, 429–434. [CrossRef]
19. Instituto Nacional de Estadística (INE), Gobierno de España. Revisión Del Padrón Municipal a 1 de Enero de 2020. Available online: https://www.ine.es (accessed on 28 May 2021).
20. Gamero, B.D.R. Mitigación del Cambio Climático en el Ciclo Integral del Agua: Aplicación al Proceso de Tratamiento de Aguas Residuales. Ph.D. Thesis, Universidad de Las palmas de Gran Canaria, Las Palmas, Spain, 2022.
21. Veza, J.M.; Rodriguez-GonzalezJuan, J. Second use for old reverse osmosis membranes: Wastewater treatment. *Desalination* **2003**, *157*, 65–72. [CrossRef]
22. Basterrechea, J.M.E. Planificación y gestión del agua. *DYNA* **2000**, *75*, 61–63.
23. León Zerpa, F.; Ramos Martín, A. Sistema de medición en continuo de bajo coste para determinar la relación entre la conductividad eléctrica "EC" y la temperatura "T" en aguas salobres. *DYNA* **2021**, *96*, 364–367.
24. Dow, N.; Gray, S.; Zhang, J.; Ostarcevic, E.; Liubinas, A.; Atherton, P.; Roeszler, G.; Gibbs, A.; Duke, M. Pilot trial of membrane distillation driven by low grade waste heat: Membrane fouling and energy assessment. *Desalination* **2016**, *391*, 30–42. [CrossRef]
25. Mazlan, N.M.; Peshev, D.; Livingston, A.G. Livingston. Energy consumption for desalination—A comparison of forward osmosis with reverse osmosis, and the potential for perfect membranes. *Desalination* **2016**, *377*, 138–151. [CrossRef]
26. Lawler, W.; Bradford-Hartke, Z.; Cran, M.J.; Duke, M.; Leslie, G.; Ladewig, B.P.; Le-Clech, P. Towards new opportunities for reuse, recycling and disposal of used reverse osmosis membranes. *Desalination* **2012**, *299*, 103–112. [CrossRef]
27. Rodriguez, J.J.; Jimenez, V.; Trujillo, O.; Veza, J.M. Reuse of reverse osmosis membranes as a filtration stage in advanced wastewater treatment. *Desalination* **2002**, *150*, 219–226. [CrossRef]
28. Espíndola, J.C.; Caianelo, M.; Scaccia, N.; Rodrigues-Silva, C.; Guimarães, J.R.; Vilar, V.J. Trace organic contaminants removal from municipal wastewater using the FluHelik reactor: From laboratory-scale to pre-pilot scale. *J. Environ. Chem. Eng.* **2021**, *9*, 105060. [CrossRef]
29. Maniakova, G.; Polo-López, M.I.; Oller, I.; Abeledo-Lameiro, M.J.; Malato, S.; Rizzo, L. Simultaneous disinfection and microcontaminants elimination of urban wastewater secondary effluent by solar advanced oxidation sequential treatment at pilot scale. *J. Hazard. Mater.* **2022**, *436*, 129134. [CrossRef] [PubMed]
30. Govardhan, B.; Fatima, S.; Madhumala, M.; Sridhar, S. Modification of used commercial reverse osmosis membranes to nanofiltration modules for the production of mineral-rich packaged drinking water. *Appl. Water Sci.* **2020**, *10*, 230. [CrossRef]

31. Zhou, J.; Chang, V.W.C.; Fane, A.G. Environmental life cycle assessment of brackish water reverse osmosis desalination for different electricity production models. *Energy Environ. Sci.* **2011**, *4*, 2267–2268. [CrossRef]

32. Garcia, R. Nanofiltration and ultrafiltration membranes from end-of-life reverse osmosis membranes. A study of recycling. Ph.D. Thesis, Universidad de Alcalá de Henares, Madrid, Spain, 2017.

33. Melian Martel, N. Universidad de las Palmas de Gran Canaria, tesis doctoral "Caracterización y evaluación del ensuciamiento en membranas de ósmosis inversa con combinación de agentes ensuaciantes", June 2021. Available online: https://accedacris.ulpgc.es/bitstream/10553/17090/4/0722378_00000_0000.pdf (accessed on 1 June 2021).

34. IAGUA.ES. Available online: https://www.iagua.es/noticias/inge-gmbh-basfs-ultrafiltration-membrane-business/ultrafiltration-uf-india (accessed on 1 June 2021).

35. Dupont Water Solutions "Data Sheet IntegraFlux SFP-2880XP Ultrafiltration Membrane". Available online: https://www.dupont.com/products/integrafluxsfp2880xp.html (accessed on 1 December 2020).

36. De Beer, D.; Stoodley, P. *Microbial Biofilms. The Prokaryotes: Applied Bacteriology and Biotechnology*; Springer: Berlin/Heidelberg, Germany, 2014; pp. 343–372. [CrossRef]

37. Flemming, H.C.; Wingender, J. The Biofilm Matrix. *Nat. Rev. Microbiol.* **2010**, *8*, 623–633. [CrossRef]

38. Dimitriou, E.; Mohamed, E.S.; Karavas, C.; Papadakis, G. Experimental comparison of the performance of two reverse osmosis desalination units equipped with different energy recovery devices. *Desalination Water Treat.* **2015**, *55*, 3019–3026. [CrossRef]

39. Dimitriou, E.; Mohamed, E.S.; Kyriakarakos, G.; Papadakis, G. Experimental investigation of the performance of a reverse osmosis desalination unit under full-and part-load operation. *Desalination Water Treat.* **2015**, *53*, 3170–3178. [CrossRef]

40. Walton, N.R.G. Electrical Conductivity and Tottal Dissolved Solids—What is Their Precise Relationship? *Desalination* **1989**, *72*, 275–292. [CrossRef]

41. Boerlage, S.; Nada, N. Algal toxin removal in seawater desalination processes. *Desalination Water Treat.* **2015**, *55*, 2575–2593. [CrossRef]

42. Pichardo-Romero, D.; Garcia-Arce, Z.P.; Zavala-Ramírez, A.; Castro-Muñoz, R. Current Advances in Biofouling Mitigation in Membranes for Water Treatment: An Overview. *Processes* **2020**, *8*, 182. [CrossRef]

43. Castro-Muñoz, R. Pressure-driven membrane processes involved in waste management in agro-food industries: A viewpoint. *AIMS Energy* **2018**, *6*, 1025–1031. [CrossRef]

44. Galanakis, C.M.; Cvejic, J.; Verardo, V.; Segura-Carretero, A. Food Use for Social Innovation by Optimizing Food Waste Recovery Strategies. In *Innovation Strategies in the Food Industry: Tools for Implementation*; Academic Press: Cambridge, MA, USA, 2016.

45. Liu, B.; Wang, D.; Yu, G.; Meng, X.; David Giraldo, J.; Thakur, V.K.; Gutiérrez, E. The History and State of Art in Membrane Technologies Tarragona, Erasmus 2005. *J. Membr. Sci.* **2013**, *16*, 1–28.

46. Kabsch-Korbutowicz, M.; Kutylowska, M. The Possibilities of Modelling the Membrane Separation Processes. *Environ. Prot. Eng.* **2008**, *34*, 15.

47. Kayvani Fard, A.; McKay, G.; Buekenhoudt, A.; Al Sulaiti, H.; Motmans, F.; Khraisheh, M.; Atieh, M. Inorganic membranes: Preparation and application for water treatment and desalination. *Materials* **2018**, *11*, 74. [CrossRef]

48. Castro-Muñoz, R. The Role of New Inorganic Materials in Composite Membranes for Water Disinfection. *Membranes* **2020**, *10*, 101. [CrossRef]